Published in Chemistry – An Asian Journal 6, issue 6, 1595-1603, 2011
which should be used for any reference to this work

Encapsulation of Pyrene-Functionalized Poly(benzyl ether) Dendrons into a Water-Soluble Organometallic Cage

Anaïs Pitto-Barry,[a] Nicolas P. E. Barry,[a] Olivier Zava,[b] Robert Deschenaux,[a] Bruno Therrien*[a]

[a] A. Pitto-Barry, N. P. E. Barry, Prof. R. Deschenaux, Dr. B. Therrien
Institut de Chimie, Université de Neuchâtel, Ave de Bellevaux 51, CH-2000, Neuchâtel (Switzerland), Fax: (+41) 32-7182511
E-mail: bruno.therrien@unine.ch

[b] Dr. O. Zava
Institut des Sciences et Ingénierie Chimique, Ecole Polytechnique Fédérale de Lausanne (EPFL), CH-1015 Lausanne (Switzerland)

Abstract: Two generations of lipophilic pyrenyl functionalized poly(benzyl ether) dendrimers (P_1 and P_2) have been synthesized. The thermal properties of the two functionalized dendrimers have been investigated, and the pyrenyl group of the dendritic molecules encapsulated in the arene–ruthenium metalla-cage, $[Ru_6(p\text{-cymene})_6(tpt)_2(donq)_3]^{6+}$ ($[\mathbf{1}]^{6+}$) (tpt = 2,4,6-tri(pyridin-4-yl)-1,3,5-triazine; donq = 5,8-dioxydo-1,4-naphthoquinonato). The host–guest properties of $[P_1\subset\mathbf{1}]^{6+}$ and $[P_2\subset\mathbf{1}]^{6+}$ were studied in solution by NMR and UV/Vis spectroscopic methods, thus allowing the determination of the affinity constants. Moreover, the cytotoxicity of these water-soluble host–guest systems was evaluated on human ovarian cancer cells.

Keywords: anticancer compounds · dendrimer · drug delivery · host–guest chemistry · metalla-cage

Introduction

Dendrimers are polymeric compounds that possess different shapes, sizes, and structures (spherical, ellipsoidal, or cylindrical), depending on the dendrimer's generation, core, and peripheral groups,[1] leading to a plethora of different physical and chemical properties.[2] Since their conception, many efforts have been made to facilitate the synthesis of these macromolecules. In particular the groups of Newkome,[3] Tomalia,[4] Fréchet,[5] and others[6] have developed numerous strategies for the preparation of dendritic systems. The versatility and the accessibility of dendrimers have led to applications in liquid-crystal chemistry,[7] as materials,[8] and also in biochemistry.[9,1b] Indeed, many examples of dendrimers being used as biological agents are known. Selected examples include antibacterial drugs based on polypropylenimine (PPI) dendrimers,[10] antiviral drugs comprising poly-(phosphorhydrazone) dendrimers with terminal phosphonic acid and alkyl chain groups,[11] as well as drug-delivery systems based on polyamidoamine (PAMAM),[4] poly-(L-lysine),[12] polyamide,[3] polypropylenimine,[13] and poly-(2,2-bis(hydroxymethyl) propionic acid (bis-MPA)[14] dendrimers. The properties of some dendrimers have been harnessed as drug carriers,[15] and their combination with metal ions has led to the discovery of new putative anticancer agents with novel modes of action.[16]

As far as we are aware, and despite considerable interest in biological applications of dendrimers, the well-known and well-documented poly(benzyl ether) dendrimers, based on benzyloxy-core with dodecanyloxy-end-groups,[17] have not been reported in this respect. The reason that these dendrimers has not been tested as biological agents probably stems from their insolubility in water, which prevents their formulation in biological media.[18]

Recently, we have reported water-soluble arene–ruthenium metalla-assemblies that are able to encapsulate planar guest molecules with[19] or without easy release of the guest.[20] Three generations of hydrophobic pyrenyl-functionalized cyanobiphenyl dendrimers were encapsulated into the hexacationic water-soluble arene–ruthenium metalla-prism, $[Ru_6(p\text{-cymene})_6(tpt)_2(donq)_3]^{6+}$ ($[\mathbf{1}]^{6+}$) (tpt = 2,4,6-tri(pyridin-4-yl)-1,3,5-triazine; donq = 5,8-dioxydo-1,4-naphthoquinonato). The cytotoxicity of the host–guest systems was evaluated on human ovarian cancer cell lines, which indicates that the metalla-cage $[\mathbf{1}]^{6+}$ was able to deliver the hydrophobic guest molecules into cancer cells.[21] Consequently, to allow poly(benzyl ether) dendrimers with dodecanyloxy-end-groups to be biologically evaluated, we have pre-

pared pyrenyl-containing dendrimers (P_n), based on 3,5-disubstituted benzyl ether repeated units functionalized at their periphery. These molecules have been fully characterized and their thermal properties studied. Moreover, the pyrenyl end-group of P_1 and P_2 has been encapsulated into the hydrophobic cavity of prism $[\mathbf{1}]^{6+}$, giving rise to water-soluble host–guest systems. The synthesis, host–guest properties, stability, and cytotoxicity of $[P_1\subset\mathbf{1}]^{6+}$ and $[P_2\subset\mathbf{1}]^{6+}$.

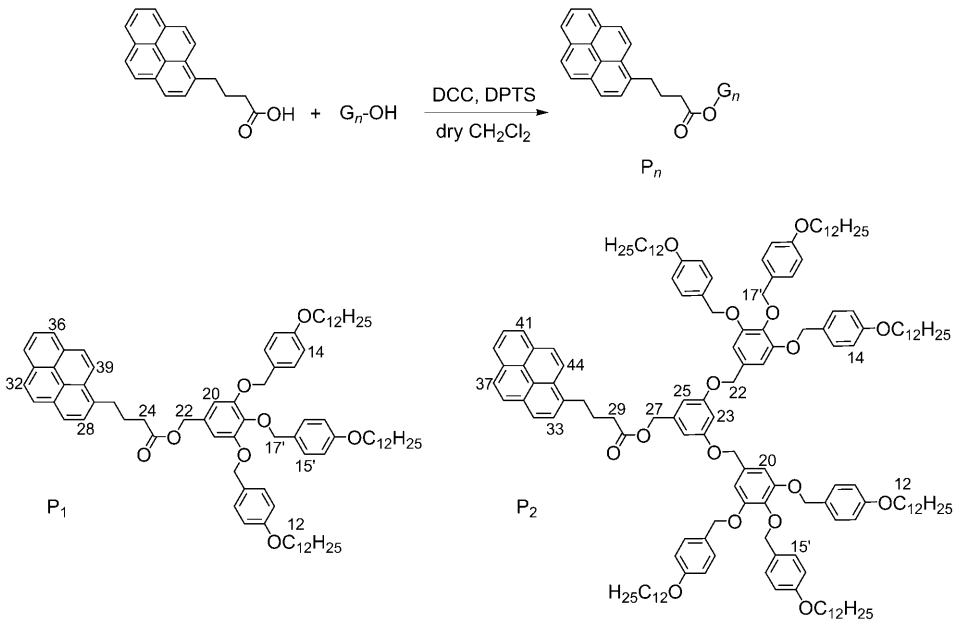

Scheme 1. Synthesis of P_1 and P_2 from 1-pyrenebutyric acid and the G_n–OH precursors.

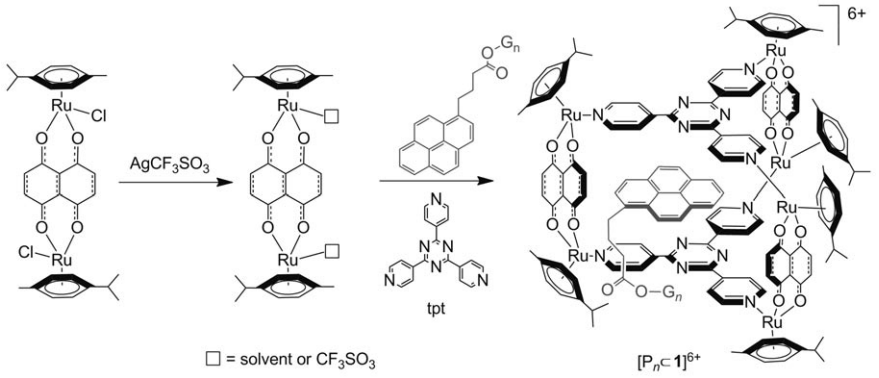

Scheme 2. Encapsulation of P_1 and P_2 in the metalla-prism $[\mathbf{1}]^{6+}$.

Results and Discussion

Two generations of dendritic precursors developed by Percec et al.,[17b] 3,4,5-tris[*p*-(*n*-dodecan-1-yloxy)benzyloxy]-benzyl alcohol (G_1–OH) and 3,5-bis{3′,4′,5′-tris[*p*-(*n*-dodecan-1-yloxy)benzyloxy]benzyloxy}benzyl alcohol (G_2–OH), were used for the synthesis of the pyrenyl-functionalized dendrimers P_1 and P_2. These two pyrenyl derivatives (P_n) were obtained in good yield by an esterification reaction between 1-pyrenebutyric acid and the dendritic precursors (G_n–OH) (Scheme 1).

The ^{1}H NMR signals for the aliphatic protons of the pyrenyl unit were used to monitor the progress of the esterification reactions. After coupling, these signals were shifted slightly upfield by up to 0.03 ppm relative to 1-pyrenebutyric acid. Moreover, the chemical environments of protons H_{22} in P_1 and H_{27} in P_2 (for numbering, see Scheme 1), were strongly modified and led to a significant downfield shift of the associated signals (0.46 and 0.48 ppm, respectively). In their $^{13}C\{^1H\}$ NMR spectra, an upfield shift was also observed for the signals of carbons C_{21} in P_1 (4.87 ppm) and C_{26} in P_2 (5.18 ppm). All chemical shifts were consistent with the formation of P_1 and P_2 and full assignments are given in the Experimental Section.

The host–guest systems $[P_n\subset\mathbf{1}]^{6+}$ were prepared using a two-step strategy (Scheme 2). The dinuclear complex [Ru_2(*p*-cymene)$_2$(donq)Cl_2] was first reacted with $AgCF_3SO_3$ to afford a dinuclear intermediate, and then 0.66 equivalent of the tpt panels and 0.33 equivalent of the guest molecule (P_n) were added to obtain the corresponding inclusion compounds. The resulting hexacationic host–guest systems were isolated in approximately 80 % yield as their triflate salts $[P_n\subset\mathbf{1}][CF_3SO_3]_6$.

The dinuclear intermediate, mentioned above, can be isolated prior to the formation of the metalla-prism. If the reaction is performed in water, the aqua complex [Ru_2(*p*-cymene)$_2$(donq)$(OH_2)_2$][CF_3SO_3]$_2$ is isolated, which has been characterized by IR and NMR spectroscopy, mass spectrometry, and by single-crystal X-ray diffraction analysis. The molecular structure of the dication [Ru_2(*p*-cymene)$_2$(donq)$(OH_2)_2]^{2+}$ is depicted in Figure 1, along with selected geometrical parameters. The dication adopts a *syn* geometry in the crystal, the required pre-orientation for construction of the metalla-prism,[22] although the existence of the *anti* isomer in solution cannot be ruled out. Indeed, an *anti* geometry was observed in the crystalline structure of the oxalato derivatives [Ru_2(hexamethylbenzene)$_2$(oxalato)-(triazolo)$_2$] and [Ru_2(*p*-cymene)$_2$(oxalato)$(CH_3OH)_2]^{2+}$,[23]

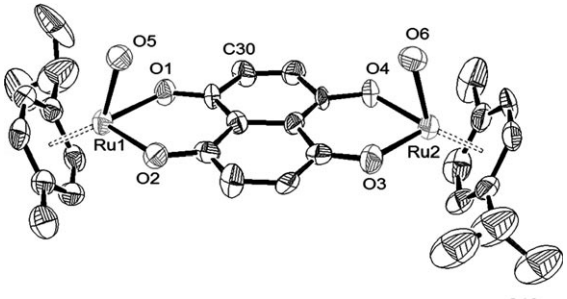

Figure 1. ORTEP drawing of $[Ru_2(p\text{-cymene})_2(donq)(OH_2)_2]^{2+}$ at the 50% probability level. Hydrogen atoms and CF_3SO_3 anions are omitted for clarity. Selected bond lengths (Å) and angles (°): Ru1–O1 2.067(10), Ru1–O2 2.017(10), Ru1–O5 2.157(6), Ru2–O3 1.993(11), Ru2–O4 2.071(9), Ru2–O6 2.150(8); O1-Ru1-O2 86.1(4), O1-Ru1-O5 81.6(3), O2-Ru1-O5 77.8(3), O3-Ru2-O4 87.2(4), O3-Ru2-O6 81.4(4), O4-Ru2-O6 81.2(3).

while a *syn* geometry was observed in $[Ru_2(p\text{-cymene})_2(ON{\cap}NO)Cl_2]$ ($ON{\cap}NO$ = 2,5-di-[2-(trifluoromethyl)-anilino]-1,4-benzoquinone).[24]

In the dinuclear complex, each ruthenium center is bound to a *para*-cymene ligand and two of the four oxygen atoms of the dianionic $OO{\cap}OO$ donq ligand. A water molecule completes the coordination sphere of the octahedral ruthenium atoms. In the structure, the ruthenium–ruthenium intramolecular separation is 8.363(1) Å, which is slightly longer than those found in analogous $ON{\cap}NO$ dinuclear complexes.[24] The presence of coordinated water molecules generates an extensive hydrogen-bonding network between the oxygen atoms of the triflate anions and the OH_2 ligands: the shortest O•••••O distance being 2.62(1) Å.

Despite obtaining crystals of the dinuclear intermediate, we were unable to grow crystals of the inclusion systems $[P_n{\subset}\mathbf{1}][CF_3SO_3]_6$ suitable for X-ray analysis. Consequently, molecular dynamic simulation using HyperChem[25] provided a 3D representation of these hexacationic host–guest systems. The simulations showed, as expected, the dendritic arm extending from the cavity with the pyrenyl moiety being encapsulated inside the prism (Figure 2). The $[P_1{\subset}\mathbf{1}]^{6+}$ and $[P_2{\subset}\mathbf{1}]^{6+}$ systems are estimated to be approximately 4.2 nm long if they are considered to be cylindrical.

The $[P_1{\subset}\mathbf{1}][CF_3SO_3]_6$ and $[P_2{\subset}\mathbf{1}][CF_3SO_3]_6$ host–guest complexes have been fully characterized by IR, UV, and NMR spectroscopy, ESI-MS, and elemental analysis. The infrared spectra of $[P_n{\subset}\mathbf{1}]^{6+}$ are dominated by absorptions of the metalla-prism $[\mathbf{1}]^{6+}$ and, in particular, by valence vibrations of the C=C and C=N skeletal modes of the tpt ligand, located between 1550–1600 cm^{-1}, and absorptions of the aromatic C–H groups at 3050 cm^{-1}. Moreover, the bands associated with the donq bridge, including the strong C=O stretching vibration (ca. 1630 cm^{-1}), are near to those observed in the dinuclear complex $[Ru_2(p\text{-cymene})_2(donq)Cl_2]$.[19a] In addition to these peaks, strong absorptions attributed to the triflate anions (1264, 1030, 639 cm^{-1}) are observed as well as peaks that may be assigned to the guest molecule, that is, the C–O stretching vibration of the aromatic ethers at 1244 cm^{-1} and C=O stretching vibrations of the ester at 1734 cm^{-1}.

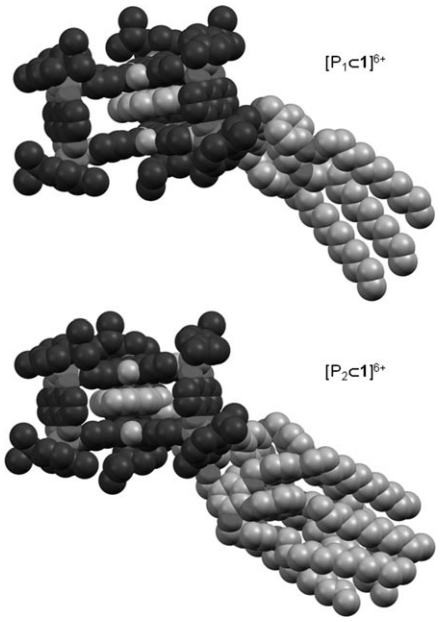

Figure 2. HyperChem simulations of $[P_1{\subset}\mathbf{1}]^{6+}$ and $[P_2{\subset}\mathbf{1}]^{6+}$, hydrogen atoms and triflate anions being omitted for clarity and carbon atoms of $[\mathbf{1}]^{6+}$ being dark grey.

The electronic absorption spectra of metalla-prism $[\mathbf{1}]^{6+}$ and the inclusion complexes $[P_n{\subset}\mathbf{1}]^{6+}$ are characterized by an intense high-energy band centered at 250 nm, which may be assigned to a localized-ligand or intraligand $\pi\rightarrow\pi^*$ transition. Two broad high-energy bands associated to metal-to-ligand charge transfer (MLCT) transitions are observed at 350 and 440 nm and two low-energy MLCT bands occurred at 640 and 700 nm. In the $[P_n{\subset}\mathbf{1}]^{6+}$ spectra, additional bands, owing to the presence of the guest molecules are observed at 317, 329, and 346 nm. The characteristic pattern of the electronic absorption spectra of $[P_n{\subset}\mathbf{1}]^{6+}$ was used to study the stability of the inclusion complexes in biological media. Absorption spectra of $[P_n{\subset}\mathbf{1}]^{6+}$ (10^{-5} M) are monitored in a solution of 10% of dimethyl sulfoxide and 90% of RPMI (Roswell Park Memorial Institute medium) 1640 with GlutaMAX™ containing 5% fetal calf serum (FCS) and antibiotics (penicillin and ciproxin). The systems did not show any signs of degradation or loss of the guest molecule, even after 24 hours at 40 °C (Figure 3). For comparison, absorption spectra of P_1 and P_2 in dichloromethane at 10^{-5} M, and absorption spectrum of $[\mathbf{1}]^{6+}$ at 10^{-5} M in a solution of 10% of dimethyl sulfoxide and 90% of RPMI are also provided in Figure 3.

The formation of $[P_n{\subset}\mathbf{1}]^{6+}$ is also monitored by ^1H NMR spectroscopy. The signals of the different protons of the pyridyl groups of the tpt panels are shifted upfield compared to the empty metalla-prism upon formation of the inclusion systems, whereas the signals of the C*H* protons of the donq bridging ligands are shifted downfield. Moreover, broadening of the signals of the tpt panels is observed, which is char-

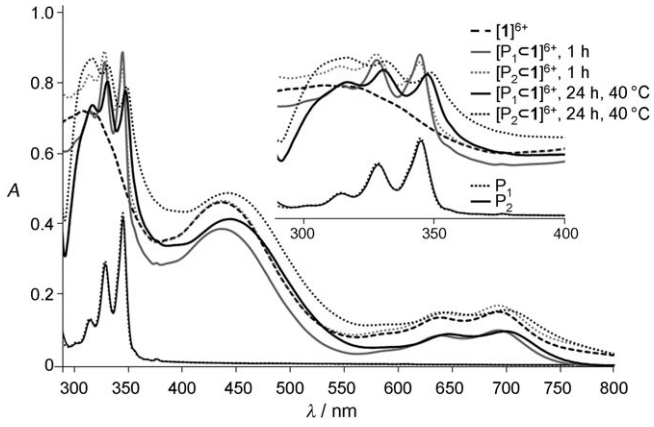

Figure 3. UV/Vis spectra of $[\mathbf{1}]^{6+}$ and $[P_n\subset\mathbf{1}]^{6+}$ (10^{-5} M concentration) in biological medium (P_1 and P_2 in CH_2Cl_2 at 10^{-5} M concentration).

acteristic of encapsulation.[20] As expected, the signals of the protons of the *para*-cymene ligands located on the periphery of the prism are not significantly affected by the presence of a guest molecule in the cavity of $[\mathbf{1}]^{6+}$. The signals of the pyrenyl moiety broadened to such an extent that they are not observed in CD_2Cl_2, in accordance with previously reported encapsulations in arene–ruthenium metalla-assemblies.[21] The signals of the CH_2 protons of the butyric chain, connecting the pyrenyl and dendritic parts, are strongly influenced by encapsulation, with an upfield shift of 0.6 ppm for the protons of the CH_2 group directly attached to the pyrenyl moiety and 0.2 ppm for the β-CH_2 group. The signals of the protons located on the dendritic arms are not influenced by encapsulation (Figure 4); similar behavior is observed in the NMR spectrum of $[P_2\subset\mathbf{1}]^{6+}$.

Under electro-spray mass spectrometry conditions the cationic host–guest complexes showed remarkable stability. The peaks corresponding to $[P_1+\mathbf{1}+(CF_3SO_3)_3]^{3+}$ and $[P_2+\mathbf{1}+(CF_3SO_3)_3]^{3+}$ are observed in the ESI mass spectra at m/z 1432.7 and 1794.6, respectively. These peaks are unambiguously assigned on the basis of their characteristic Ru_6 isotope patterns (Figure 5).

Thermal Studies

The thermal properties of the pyrenyl derivatives P_1 and P_2 have been investigated by polarized optical microscopy and differential scanning calorimetry. During the first heating run, viscous and birefringent fluids are observed between 53 and 60 °C for P_1 and between 59 and 74 °C for P_2 (Figure 6).

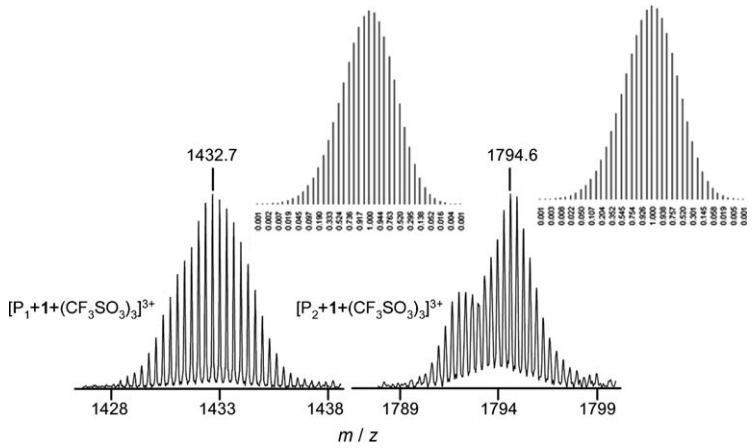

Figure 5. ESI-MS of the peak envelopes corresponding to $[P_1+\mathbf{1}+(CF_3SO_3)_3]^{3+}$ and $[P_2+\mathbf{1}+(CF_3SO_3)_3]^{3+}$ and simulations of their isotopic pattern.

However, no typical textures are obtained which prevented the identification of the mesophases. From consideration of the nature and structure of P_1 and P_2, the mesophases could be of columnar type,[17b] although this can only be confirmed by X-ray studies. The texture observed for P_2 is presented in Figure 7 as an illustrative example. On the other hand, upon heating, both host–guest systems

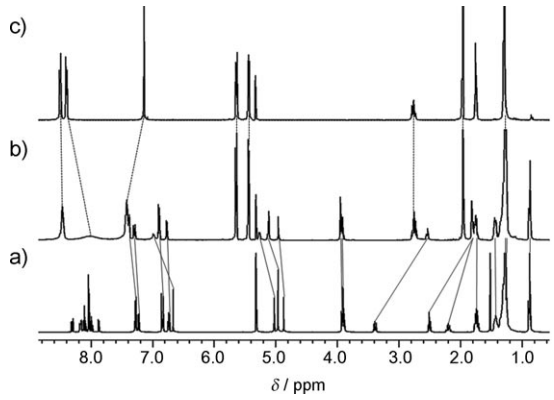

Figure 4. ^{1}H NMR spectra of P_1 (a), $[P_1\subset\mathbf{1}][CF_3SO_3]_6$ (b) and $[\mathbf{1}][CF_3SO_3]_6$ (c) in CD_2Cl_2 at 21 °C.

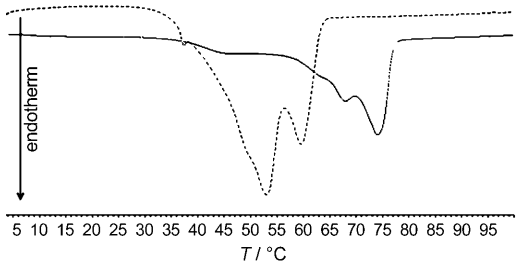

Figure 6. Differential scanning calorimetry thermograms of P_1 (-----) and P_2 (——) recorded during the first heating run.

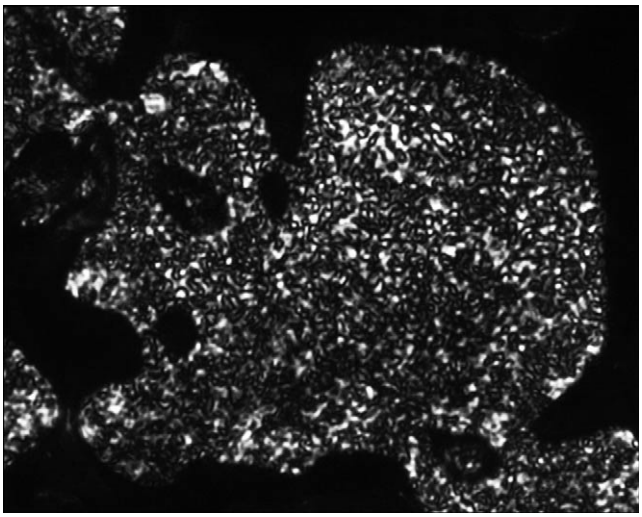

Figure 7. A thermal-polarized optical micrograph of the texture displayed by P_2 in the unidentified phase upon heating the sample from the solid state to 66 °C.

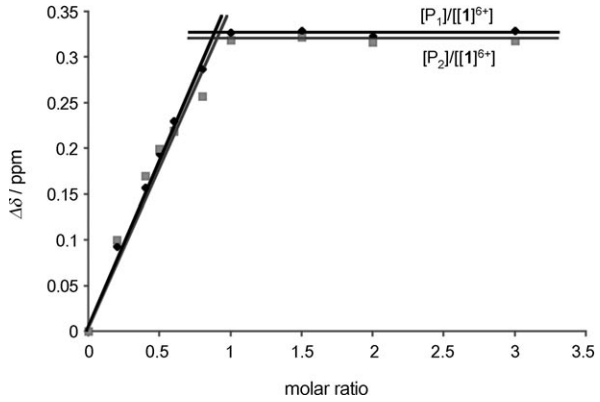

Figure 8. ^{1}H NMR chemical-shift changes for the H_β proton of the tpt ligands vs. the molar ratio of P_1 (◆) and P_2 (■) to $[\mathbf{1}]^{6+}$ (4.0 mM) in CD_2Cl_2 at 21 °C.

$[P_1\subset\mathbf{1}][CF_3SO_3]_6$ and $[P_2\subset\mathbf{1}][CF_3SO_3]_6$ show decomposition (> 200 °C) under polarized optical microscopy.

Host—Guest Studies

With the stability of the inclusion systems confirmed, the host–guest properties of the systems have been further studied in solution by ^{1}H NMR and UV/Vis spectroscopy. ^{1}H NMR titrations of P_1 and P_2 in the presence of $[\mathbf{1}]^{6+}$ are performed in CD_2Cl_2 at room temperature. Upon gradual addition of the guest molecule P_1 or P_2 (0.1–3.0 equivalents) to a CD_2Cl_2 solution of $[\mathbf{1}][CF_3SO_3]_6$ (4.0 mM), chemical changes to some of the protons of both the host and the guest are observed in the ^{1}H NMR spectrum. These changes indicate that rapid inclusion of the guest molecule into the cavity of $[\mathbf{1}]^{6+}$ takes place, as previously observed with $[\text{pyrene}\subset\mathbf{1}][CF_3SO_3]_6$.[19a] Plots of the chemical shifts ($\Delta\delta$) for the H_β proton of the tpt ligands versus the molar ratio of P_1 or P_2 to the prism $[\mathbf{1}]^{6+}$ indicate a 1:1 stoichiometry of the host–guest systems because no changes to the chemical shifts are noticed after reaching a 1:1 stoichiometry (Figure 8).[26]

From these plots, stability constants of association (K_a) have been estimated by using the non-linear least-square fitting program winEQNMR2[27] (see Table 1). The binding free energies ($\Delta G°$) for $[P_1\subset\mathbf{1}]^{6+}$ and $[P_2\subset\mathbf{1}]^{6+}$ are determined from the corresponding association constants obtained at 21 °C in CD_2Cl_2 and, in both cases, the values of $\Delta G°$ are inferior to -6.19 kcal mol^{-1}. To confirm the values of K_a and $\Delta G°$ for $[P_1\subset\mathbf{1}]^{6+}$ and $[P_2\subset\mathbf{1}]^{6+}$, the thermodynamic properties of the host–guest systems have been also studied by UV/Vis spectroscopy. Aliquots of a CH_2Cl_2 solution of guest molecule P_n are added to a CH_2Cl_2 solution of $[\mathbf{1}][CF_3SO_3]_6$ ($[P_n]/[\mathbf{1}]^{6+} = 0$–2 equiv), at 21 °C. Based on changes to the absorbance and applying the Rose and Drago equation,[28] the association constants of $[P_1\subset\mathbf{1}]^{6+}$ and $[P_2\subset\mathbf{1}]^{6+}$ are estimated (Table 1). This method is widely used to study binding phenomena, in particular for 1:1 host–guest systems.[29] The K_a values for $[P_1\subset\mathbf{1}]^{6+}$ and $[P_2\subset\mathbf{1}]^{6+}$ obtained using UV/Vis spectroscopy are consistent with the values estimated by ^{1}H NMR titrations.

Cytotoxicity Studies

Metal-based drugs are widely used in clinical applications; notably, platinum compounds are used for the treatment of cancer,[30] although ruthenium compounds are now progressing through clinical trials.[31] In addition to the classical ruthenium compounds in clinical trials, organometallic arene–ruthenium(II) compounds are attracting considerable interest as antitumor agents.[32] One of the main limitations of metal drugs is their lack of selectivity, and consequently methods to target such drugs for tumor tissue could improve their therapeutic index by reducing damage to healthy tissue and lowering drug side-effects. Dendrimers are interesting drug candidates[9a] because their macroscopic properties

Table 1. Association constants (K_a) and free energies ($\Delta G°$) for the encapsulation of P_1 and P_2 in $[\mathbf{1}]^{6+}$, determined by ^{1}H NMR titration (CD_2Cl_2 at 21 °C; 4.0 mM concentration of $[\mathbf{1}]^{6+}$) and UV/Vis spectroscopy (CH_2Cl_2 at 21 °C).

	K_a [10^4 M^{-1}]	$\Delta G°$ [kcal mol^{-1}]
NMR data		
$[P_1\subset\mathbf{1}]^{6+}$	4.2	−6.30
$[P_2\subset\mathbf{1}]^{6+}$	3.5	−6.19
UV/Vis data		
$[P_1\subset\mathbf{1}]^{6+}$	4.9	−6.39
$[P_2\subset\mathbf{1}]^{6+}$	3.9	−6.25

Table 2. IC_{50} values of P_n, $[P_n\subset\mathbf{1}][CF_3SO_3]_6$, $[\mathbf{1}][CF_3SO_3]_6$ and cisplatin on human ovarian A2780 and A2780cisR cell lines.

	A2780 [μM]	A2780cisR [μM]
P_1	ND	ND
P_2	ND	ND
$[P_1\subset\mathbf{1}][CF_3SO_3]_6$	2.4 (±0.5)	2.9 (±0.7)
$[P_2\subset\mathbf{1}][CF_3SO_3]_6$	2.5 (±0.8)	3.2 (±0.9)
$[\mathbf{1}][CF_3SO_3]_6$	3.1 (±1.0)	4.6 (±0.5)
cisplatin	1.6 (±0.6)	8.6 (±0.6)

take advantage of passive targeting of tumors via enhanced permeability and retention effect.[33] Essentially, the normal endothelial layer surrounding the blood vessels feeding healthy cells restricts the size of molecules that can diffuse from the blood, whereas the endothelial layer of blood vessels in diseased tissues is more porous, providing access for macromolecules to the surrounding cancer cells. In addition, because diseased tissue does not usually have a lymphatic drainage system, once macromolecules have entered, they are retained. Indeed, metallo-dendrimers have been shown to have promising anticancer properties.[16a,34]

Although poly(benzyl ether)-type dendrons have been used to functionalize metal nanoparticles,[35] and have been connected with platinum,[36] to the best of our knowledge the use of such dendrimers as anticancer agents has not been reported. The cytotoxicity of the water-soluble host–guest systems $[P_n\subset\mathbf{1}][CF_3SO_3]_6$, the pyrenyl-containing dendrimers P_1 and P_2 and the empty metalla-cage $[\mathbf{1}][CF_3SO_3]_6$, have been evaluated against A2780 (cisplatin sensitive) and A2780cisR (cisplatin resistant) human ovarian cancer cells. Their cytotoxicities, in comparison to cisplatin, are presented in Table 2.

The two P_n dendrimers showed no cytotoxic effects on the cell lines, presumably owing to their poor solubility in water. The metalla-cage $[\mathbf{1}]^{6+}$ is water-soluble as well as the host–guest systems $[P_n\subset\mathbf{1}]^{6+}$ and in the A2780 cell line they all exhibit a comparable cytotoxic effect. The cytotoxicities of $[\mathbf{1}]^{6+}$ and $[P_n\subset\mathbf{1}]^{6+}$ in the cisplatin-resistant cell line are essentially unchanged from the sensitive cell line. This similarity is not unexpected, because the targets and resistance mechanisms for arene–ruthenium compounds are believed to be distinct from those of cisplatin.[37] Despite the high stability of the host–guest systems in biological media, it is not clear if the guest is released or not after cellular internalization of the host–guest systems. Nevertheless, it is worth noting that 'per metal' $[\mathbf{1}]^{6+}$ and $[P_n\subset\mathbf{1}]^{6+}$ are less cytotoxic than cisplatin, but caution should be applied when making this type of comparison as ruthenium compounds tend to be better tolerated by the body.[38]

Conclusions

Poly(benzyl ether)-type dendrimers with dodecanyloxy-end-groups functionalized with a pyrenyl moiety were used to generate host–guest systems in which the pyrenyl ring was encapsulated within a hydrophilic hexanuclear metalla-prism whilst the dendritic arm was standing out. The dendritic host–guest systems $[P_1\subset\mathbf{1}]^{6+}$ and $[P_2\subset\mathbf{1}]^{6+}$ were shown to exhibit similar cytotoxicities to those of the metalla-prism alone, which suggests that the dendrimers do not have a detrimental effect on the in vitro activity, at least in the ovarian cancer cell lines studied herein, and should help to target tumor tissue in vivo by the enhanced permeability and retention effect.

Experimental Section

2,4,6-Tris(4-pyridyl)-1,3,5-triazine (tpt),[39] $[Ru_2(p\text{-cymene})_2(donq)Cl_2]$,[19a] 4-(dimethylamino)pyrimidium *para*-toluenesulfonate,[40] G_1–OH and G_2–OH[17b] were prepared according to published methods. 1-Pyrenebutyric acid and all other reagents were commercially available (Sigma–Aldrich) and used as received. ^1H and $^{13}C\{^1H\}$ NMR spectra were recorded on a Bruker AMX 400 spectrometer using the residual protonated solvent as an internal standard (CD_2Cl_2: $\delta_H = 5.32$ ppm). Infrared spectra were recorded as KBr pellets on a Perkin–Elmer FTIR 1720 X spectrometer. UV/Vis absorption spectra were recorded on a Uvikon 930 spectrophotometer using precision cells made of quartz (1 cm). Microanalyses were performed at the Mikroelementarisches Laboratorium, ETH Zürich (Switzerland). Electrospray ionisation mass spectra were obtained in positive-ion mode on a Bruker FTMS 4.7T BioAPEX II mass spectrometer. Column chromatography used silica gel 60 (0.063–0.200 mm, Brunschwig). Transition temperatures and enthalpies were determined on a Mettler–Toledo DSC1 STAR^e System differential-scanning calorimeter at a rate of 10 °C min^{-1} under N_2. Optical studies were made using a Zeiss-Axioskop polarising microscope equipped with a Linkam THMS-600 variable-temperature stage.

Synthesis of Pyrenyl-Containing Dendrimers P1 and P2

N,N′-dicyclohexylcarbodiimide (100 mg, 0.48 mmol) and 4-(dimethylamino)pyrimidium *para*-toluenesulfonate (45 mg, 0.16 mmol) were added to a mixture of dendrimer (G_1–OH, 361 mg; G_2–OH, 665 mg; 0.32 mmol) and 1-pyrenebutyric acid (93 mg, 0.32 mmol) in dry CH_2Cl_2 (30 mL) at 0 °C. The mixture was allowed to warm to RT and stirred for 24 h. The solvent was removed and the residue purified by column chromatography on silica gel (CH_2Cl_2). The solvent was then evaporated under reduced pressure and the isolated product dried under vacuum, dissolved in CH_2Cl_2 (ca. 3 mL), and precipitated with cold MeOH (ca. 80 mL). After 16 h at 5 °C, the solid was filtered and dried under vacuum.

P_1: Yield = 272 mg, 86 %. UV/Vis (1.0×10^{-5} M, CH_2Cl_2): λ_{max} 237 nm ($\varepsilon = 0.71\times10^5\,M^{-1}cm^{-1}$), λ_{max} 244 nm ($\varepsilon = 0.82\times10^5\,M^{-1}cm^{-1}$), λ_{max} 267 nm ($\varepsilon = 0.34\times10^5\,M^{-1}cm^{-1}$), λ_{max} 277 nm ($\varepsilon = 0.56\times10^5\,M^{-1}cm^{-1}$), λ_{max} 314 nm ($\varepsilon = 0.14\times10^5\,M^{-1}cm^{-1}$), λ_{max} 328 nm ($\varepsilon = 0.30\times10^5\,M^{-1}cm^{-1}$), λ_{max} 345 nm ($\varepsilon = 0.43\times10^5\,M^{-1}cm^{-1}$). IR (KBr): $\tilde{\nu}$ = 3039 (w, CH_{aryl}), 2920 (s, CH_2), 2851 (s, CH_3), 1728 (s, C=O), 1105 cm^{-1} (m, C–O). ^1H NMR (400 MHz, CD_2Cl_2): δ = 8.30 (d, $^3J_{H-H}$ = 9.3 Hz, 1H, H^{28}), 8.17 (d, $^3J_{H-H}$ = 7.5 Hz, 1H, H^{34}), 8.16 (d, $^3J_{H-H}$ = 6.7 Hz, 1H, H^{36}), 8.12 (d, $^3J_{H-H}$ = 8.0 Hz, 1H, H^{38}), 8.10 (d, 1H, H^{29}), 8.04 (s, 2H, H^{31} and H^{32}), 8.00 (t, 1H, H^{35}), 7.87 (d, 1H, H^{39}), 7.28 (d, $^3J_{H-H}$ = 8.6 Hz, 4H, H^{15}), 7.23 (d, $^3J_{H-H}$ = 8.6 Hz, 2H, $H^{15'}$), 6.84 (d, 4H, H^{14}), 6.73 (d, 2H, $H^{14'}$), 6.67 (s, 2H, H^{20}), 5.03 (s, 2H, H^{22}), 4.97 (s, 4H, H^{17}), 4.88 (s, 2H, $H^{17'}$), 3.91 (t, $^3J_{H-H}$ = 6.6 Hz, 4H, H^{12}), 3.90 (t, $^3J_{H-H}$ = 6.5 Hz, 2H, $H^{12'}$), 3.40 (m, 2H, H^{26}), 2.51 (t, $^3J_{H-H}$ = 7.2 Hz, 2H, H^{24}), 2.20 (m, 2H, H^{25}), 1.75 (m, 6H, H^{11} and $H^{11'}$), 1.42 (m, 6H, H^{10}

and $H^{10'}$), 1.30 (m, 48H, $H_{aliphatic}$), 0.88 ppm (t, $^3J_{H-H}=6.8$ Hz, 9H, H^1 and $H^{1'}$). $^{13}C\{^1H\}$ NMR (100 MHz, CD_2Cl_2): $\delta=173.4$ (C^{23}), 159.5 (C^{13}), 159.4 ($C^{13'}$), 153.4 (C^{19}), 138.5 (C^{18}), 136.4 (C^{27}), 132.1 (C^{21}), 131.8 (C^{33}), 131.3 (C^{40}), 130.5 ($C^{15'}$), 130.4 (C^{30}), 130.3 ($C^{16'}$), 129.7 (C^{15}), 129.3 (C^{16}), 129.2 (C^{37}), 127.9 (C^{31}), 127.8 (C^{29}), 127.7 (C^{39}), 127.1 (C^{32}), 126.3 (C^{35}), 125.4 (C^{41} and C^{42}), 125.3 (C^{36}), 125.2 (C^{34}), 125.1 (C^{38}), 123.8 (C^{28}), 114.8 (C^{14}), 114.4 ($C^{14'}$), 107.9 (C^{20}), 75.1 ($C^{17'}$), 71.3 (C^{17}), 68.5 (C^{12}), 68.4 ($C^{12'}$), 66.6 (C^{22}), 34.3 (C^{24}), 33.1 (C^{26}), 32.4 (C^3 and $C^{3'}$), 30.3 (C_{aliph}), 30.2 (C_{aliph}), 30.1 (C_{aliph}), 30.0 (C_{aliph}), 29.9 (C_{aliph}), 29.8 (C_{aliph}), 29.7 (C_{aliph}), 29.6 (C_{aliph}), 29.5 (C_{aliph}), 27.3 (C^{25}), 26.5 ($C^{10'}$), 26.4 (C^{10}), 23.1 (C^2 and $C^{2'}$), 14.3 ppm (C^1 and $C^{1'}$). ESI-MS: m/z 1271.8 $[P_1+Na]^+$. Elemental analysis calcd (%) for $C_{84}H_{112}O_8$: C 80.73, H 9.03; found: C 80.75, H 9.05.

P_2: Yield = 527 mg, 70%. UV/Vis (1.0×10^{-5} M, CH_2Cl_2): λ_{max} 236 nm ($\varepsilon=1.14\times10^5\,M^{-1}cm^{-1}$), λ_{max} 244 nm ($\varepsilon=0.96\times10^5\,M^{-1}cm^{-1}$), λ_{max} 267 nm ($\varepsilon=0.37\times10^5\,M^{-1}cm^{-1}$), λ_{max} 277 nm ($\varepsilon=0.61\times10^5\,M^{-1}cm^{-1}$), λ_{max} 314 nm ($\varepsilon=0.13\times10^5\,M^{-1}cm^{-1}$), λ_{max} 328 nm ($\varepsilon=0.29\times10^5\,M^{-1}cm^{-1}$), λ_{max} 345 nm ($\varepsilon=0.42\times10^5\,M^{-1}cm^{-1}$). IR (KBr): $\tilde{\nu}=3040$ (w, CH_{aryl}), 2922 (s, CH_2), 2851 (s, CH_3), 1735 (s, C=O), 1107 cm^{-1} (m, C–O). ^1H NMR (400 MHz, CD_2Cl_2): $\delta=8.28$ (d, $^3J_{H-H}=9.2$ Hz, 1H, H^{33}), 8.14 (d, $^3J_{H-H}=7.5$ Hz, 1H, H^{39}), 8.13 (d, $^3J_{H-H}=5.4$ Hz, 1H, H^{41}), 8.09 (d, $^3J_{H-H}=7.9$ Hz, 1H, H^{43}), 8.06 (d, 1H, H^{34}), 8.00 (s, 2H, H^{36} and H^{37}), 7.97 (t, 1H, H^{40}), 7.85 (d, 1H, H^{44}), 7.30 (d, $^3J_{H-H}=8.6$ Hz, 8H, H^{15}), 7.23 (d, $^3J_{H-H}=8.6$ Hz, 4H, $H^{15'}$), 6.86 (d, 8H, H^{14}), 6.74 (d, 4H, $H^{14'}$), 6.72 (s, 4H, H^{20}), 6.64 (d, $^4J_{H-H}=2.1$ Hz, 2H, H^{25}), 6.58 (t, 1H, H^{23}), 5.10 (s, 2H, H^{27}), 4.96 (s, 8H, H^{17}), 4.94 (s, 4H, H^{22}), 4.88 (s, 4H, $H^{17'}$), 3.93 (t, $^3J_{H-H}=7.0$ Hz, 12H, H^{12}), 3.91 (t, $^3J_{H-H}=7.0$ Hz, 6H, $H^{12'}$), 3.38 (m, 2H, H^{31}), 2.53 (t, $^3J_{H-H}=7.1$ Hz, 2H, H^{29}), 2.20 (m, 2H, H^{30}), 1.76 (m, 12H, H^{11} and $H^{11'}$), 1.45 (m, 12H, H^{10} and $H^{10'}$), 1.32 (m, 96H, $H_{aliphatic}$), 0.88 ppm (t, $^3J_{H-H}=6.8$ Hz, 18H, H^1 and $H^{1'}$). $^{13}C\{^1H\}$ NMR (100 MHz, CD_2Cl_2): $\delta=173.4$ (C^{28}), 160.5 (C^{24}), 159.6 (C^{13}), 159.4 ($C^{13'}$), 153.5 (C^{19}), 139.2 (C^{26}), 138.3 (C^{18}), 136.4 (C^{32}), 132.7 (C^{21}), 131.8 (C^{38}), 131.3 (C^{45}), 130.5 ($C^{15'}$), 130.4 ($C^{16'}$ and C^{35}), 129.7 (C^{15}), 129.3 (C^{16}), 129.2 (C^{42}), 127.9 (C^{36}), 127.8 (C^{34}), 127.7 (C^{44}), 127.1 (C^{37}), 126.3 (C^{40}), 125.4 (C^{46} and C^{47}), 125.3 (C^{41} and C^{39}), 125.2 (C^{43}), 123.8 (C^{33}), 114.8 (C^{14}), 114.4 ($C^{14'}$), 107.5 (C^{25}), 107.3 (C^{20}), 102.1 (C^{23}), 75.1 ($C^{17'}$), 71.3 (C^{17}), 70.7 (C^{22}), 68.5 (C^{12}), 68.4 ($C^{12'}$), 66.4 (C^{27}), 34.3 (C^{29}), 33.1 (C^{31}), 32.4 (C^3 and $C^{3'}$), 30.2 (C_{aliph}), 30.1 (C_{aliph}), 30.0 (C_{aliph}), 29.9 (C_{aliph}), 29.8 (C_{aliph}), 29.7 (C_{aliph}), 29.6 (C_{aliph}), 27.3 (C^{30}), 26.5 (C^{10} and $C^{10'}$), 23.1 (C^2 and $C^{2'}$), 14.3 ppm (C^1 and $C^{1'}$). ESI-MS: m/z 2355.6 $[(P_2+1)+Na]^+$. Elemental analysis calcd (%) for $C_{155}H_{214}O_{16}$: C 79.78, H 9.24; found: C 80.02, H 9.27.

Synthesis of $[Ru_2(p\text{-cymene})_2(donq)(OH_2)_2][CF_3SO_3]_2$

A mixture of $Ag(CF_3SO_3)$ (144 mg, 0.56 mmol) and $[Ru_2(p\text{-cymene})_2(donq)Cl_2]$ (204 mg, 0.28 mmol), in MeOH (80 mL) was stirred at RT for 6 h. After filtration of AgCl, the filtrate was evaporated to dryness to give a green solid. Recrystallisation from CH_2Cl_2/H_2O afforded nicely shaped green crystals of $[Ru_2(p\text{-cymene})_2(donq)(OH_2)_2][CF_3SO_3]_2$.

Yield = 202 mg, 73%. IR (KBr): $\tilde{\nu}=3070$ (w, CH_{aryl}), 1536 (s, C=O), 1268 cm^{-1} (s, CF_3). ^1H NMR (400 MHz, D_2O): $\delta=7.22$ (s, 4H, H_{donq}), 5.71 (d, $^3J_{H-H}=6.8$ Hz, 4H, H_{cym}), 5.48 (d, 4H, H_{cym}), 2.68 (sept, $^3J_{H-H}=5.8$ Hz, 2H, $CH(CH_3)_2$), 2.12 (s, 6H, CH_3), 1.19 ppm (d, 12H, $CH(CH_3)_2$). $^{13}C\{^1H\}$ NMR (100 MHz, D_2O): $\delta=173.1$ (CO), 139.2 (CH_{donq}), 114.7 (C_{donq}), 102.1 (C_{cym}), 10.1 (C_{cym}), 84.3 (CH_{cym}), 82.9 (CH_{cym}), 30.6 ($CH(CH_3)_2$), 21.2 ($CH(CH_3)_2$), 17.5 ppm (CH_3). ESI-MS: m/z 808.0 [(M-2)-(H_2O)-$CF_3SO_3]^+$. Elemental analysis calcd (%) for $C_{32}H_{36}F_6O_{12}Ru_2S_2$: C 38.71, H 3.65; found: C 38.68, H 3.63.

X-ray Data for $[Ru_2(p\text{-cymene})_2(donq)(OH_2)_2][CF_3SO_3]_2$

$C_{32}H_{36}F_6O_{12}Ru_2S_2$, $M=992.89$, Monoclinic, space group $P\,n$ (No. 7), cell parameters $a=12.0325(15)$, $b=12.8232(10)$, $c=13.2027(16)$ Å, $\beta=111.401(9)°$, $V=1896.7(4)$ Å^3, $T=173(2)$ K, $Z=2$, $\rho_{cald}=1.738$ g cm^{-3}, λ ($Mo_{K\alpha}$) = 0.71073 Å, 9031 reflections measured, 4269 unique ($R_{int}=0.1283$) which were used in all calculations. The structure was solved by direct method (SHELXL-97)[41] and refined by full-matrix least-squares methods on F^2 with 463 parameters. $R_1=0.0635$ ($I>2\sigma(I)$) and $wR_2=0.1621$, GOF = 0.829; max./min. residual density 1.036/−1.069 e Å^{-3}. Figure 1 was drawn with ORTEP-3.[42] CCDC 810124 $[Ru_2(p\text{-cymene})_2(donq)(OH_2)_2][CF_3SO_3]_2$ contains the supplementary crystallographic data for this paper. These data can be obtained free of charge from the Cambridge Crystallographic Data Centre via www.ccdc.cam.ac.uk/data_request/cif.

Synthesis of $[P_n\subset\mathbf{1}][CF_3SO_3]_6$

A mixture of $Ag(CF_3SO_3)$ (144 mg, 0.56 mmol) and $[Ru_2(p\text{-cymene})_2(donq)Cl_2]$ (198 mg, 0.27 mmol), in MeOH (80 mL) was stirred at RT for 6 h. Then the guest molecule (P_1, 114 mg; P_2, 213 mg; 0.09 mmol) and tpt (56 mg, 0.18 mmol) were added and the solution was stirred at 60 °C for 24 h. The solvent was removed under vacuum and the residue dissolved in CH_2Cl_2 (40 mL), and filtered to eliminate AgCl. After evaporation of CH_2Cl_2, the solid was washed with diethyl ether and pentane before being dried under vacuum.

$[P_1\subset\mathbf{1}][CF_3SO_3]_6$: Yield = 389 mg, 82%. UV/Vis (1.0×10^{-5} M, CH_2Cl_2): λ_{max} 249 nm ($\varepsilon=2.44\times10^5\,M^{-1}cm^{-1}$), λ_{max} 278 nm ($\varepsilon=1.17\times10^5\,M^{-1}cm^{-1}$), λ_{max} 321 nm ($\varepsilon=0.71\times10^5\,M^{-1}cm^{-1}$), λ_{max} 331 nm ($\varepsilon=0.83\times10^5\,M^{-1}cm^{-1}$), λ_{max} 345 nm ($\varepsilon=0.89\times10^5\,M^{-1}cm^{-1}$), λ_{max} 440 nm ($\varepsilon=0.39\times10^5\,M^{-1}cm^{-1}$), λ_{max} 643 nm ($\varepsilon=0.09\times10^5\,M^{-1}cm^{-1}$), λ_{max} 701 nm ($\varepsilon=0.10\times10^5\,M^{-1}cm^{-1}$). IR (KBr): $\tilde{\nu}=3050$ (w, CH_{aryl}), 1734 (s, $C{=}O_{ester}$), 1630 (s, $C{=}O_{donq}$), 1595 (s, $C{=}C_{tpt}$), 1558 (s, $C{=}N_{tpt}$), 1264 (s, CF_3), 1242 (s, C-$O_{aromatic\ ether}$), 1030 (s, CF_3), 640 cm^{-1} (s, CF_3). ^1H NMR (400 MHz, CD_2Cl_2): $\delta=8.46$ (m, 12H, H_α), 8.01 (m, 12H, H_β), 7.42 (s, 12H, H_{donq}), 7.38 (d, $^3J_{H-H}=8.4$ Hz, 4H, H^{15}), 7.29 (d, $^3J_{H-H}=8.4$ Hz, 2H, $H^{15'}$), 6.99 (s, 2H, H^{20}), 6.89 (d, 4H, H^{14}), 6.77 (d, 2H, $H^{14'}$), 5.64 (d, $^3J_{H-H}=6.3$ Hz, 12H, H_{cym}), 5.44 (d, 12H, H_{cym}), 5.27 (s, 2H, H^{22}), 5.12 (s, 4H, H^{17}), 4.96 (s, 2H, $H^{17'}$), 3.95 (t, $^3J_{H-H}=6.5$ Hz, 4H, H^{12}), 3.92 (t, $^3J_{H-H}=5.5$ Hz, 2H, $H^{12'}$), 2.75 (sept, $^3J_{H-H}=7.0$ Hz, 6H, $CH(CH_3)_2$), 2.54 (m, 2H, H^{26}), 1.96 (s, 18H, CH_3), 1.81 (m, 4H, H^{24} and H^{25}), 1.76 (m, 6H, H^{11} and $H^{11'}$), 1.45 (m, 6H, H^{10} and $H^{10'}$), 1.28 (m, 84H, $H_{aliphatic}$ and $CH(CH_3)_2$), 0.88 ppm (m, 9H, H^1 and $H^{1'}$). $^{13}C\{^1H\}$ NMR (100 MHz, CD_2Cl_2): $\delta=173.7$ (C^{23}), 171.3 (CO), 169.0 (C_{tpt}), 159.6 (C^{13}), 159.5 ($C^{13'}$), 153.5 (C_α), 153.0 (C^{19}), 143.8 (C_{tpt}), 138.4 (C^{18}), 138.1 (CH_{donq}), 132.0 (C_{pyr}), 130.7 ($C^{15'}$), 130.2 ($C^{16'}$), 129.8 (C^{15}), 129.3 (C^{16}), 127.9 (C_{pyr}), 127.6 (CH_{pyr}), 127.4 (CH_{pyr}), 126.7 (C_{pyr}), 126.3 (C_β), 114.8 (C^{14}), 114.5 ($C^{14'}$), 112.0 (C_{donq}), 108.2 (C^{20}), 104.2 (C_{cym}), 100.7 (C_{cym}), 85.2 (CH_{cym}), 83.0 (CH_{cym}), 75.3 ($C^{17'}$), 71.5 (C^{17}), 68.5 (C^{12}), 68.4 ($C^{12'}$), 66.9 (C^{22}), 32.3 (C^{26}), 31.1 (C^3 and $C^{3'}$), 30.1 ($CH(CH_3)_2$), 29.8 (C_{aliph}), 26.4 (C^{10} and $C^{10'}$), 23.1 (C^2 and $C^{2'}$), 22.4 ($CH(CH_3)_2$), 17.4 (CH_3), 14.3 ppm (C^1 and $C^{1'}$). ESI-MS: m/z 1432.7 $[P_1+\mathbf{1}+(CF_3SO_3)_3]^{3+}$. Elemental analysis calcd (%) for $C_{216}H_{232}F_{18}N_{12}O_{38}Ru_6S_6$: C 54.68, H 4.93, N 3.54; found: C 54.93, H 5.19, N 3.54.

$[P_2\subset\mathbf{1}][CF_3SO_3]_6$: Yield = 484 mg, 83%. UV/Vis (1.0×10^{-5} M, CH_2Cl_2): λ_{max} 245 nm ($\varepsilon=2.78\times10^5\,M^{-1}cm^{-1}$), λ_{max} 278 nm ($\varepsilon=1.18\times10^5\,M^{-1}cm^{-1}$), λ_{max} 319 nm ($\varepsilon=0.81\times10^5\,M^{-1}cm^{-1}$), λ_{max} 329 nm ($\varepsilon=0.88\times10^5\,M^{-1}cm^{-1}$), λ_{max} 345 nm ($\varepsilon=0.85\times10^5\,M^{-1}cm^{-1}$), λ_{max} 440 nm ($\varepsilon=0.47\times10^5\,M^{-1}cm^{-1}$), λ_{max} 643 nm ($\varepsilon=0.15\times10^5\,M^{-1}cm^{-1}$), λ_{max} 701 nm ($\varepsilon=0.17\times10^5\,M^{-1}cm^{-1}$). IR (KBr): $\tilde{\nu}=3050$ (w, CH_{aryl}), 1733 (s, $C{=}O_{ester}$), 1630 (s, $C{=}O_{donq}$), 1582 (s, $C{=}C_{tpt}$), 1564 (s, $C{=}N_{tpt}$), 1264 (s, CF_3), 1242 (s, C-$O_{aromatic\ ether}$), 1030 (s, CF_3), 639 cm^{-1} (s, CF_3). ^1H NMR (400 MHz, CD_2Cl_2): $\delta=8.53$ (m, 12H, H_α), 8.29 (m, 12H, H_β), 7.34 (s, 12H, H_{donq}), 7.32 (m, 8H, H^{15}), 7.23 (d, $^3J_{H-H}=8.5$ Hz, 2H, $H^{15'}$), 6.87 (d, $^3J_{H-H}=8.8$ Hz, 8H, H^{14}), 6.85 (s, 4H, H^{20}), 6.74 (d, 4H, $H^{14'}$), 6.73 (m, 2H, H^{25}), 6.70 (t, 1H, H^{23}), 5.64 (d, $^3J_{H-H}=6.3$ Hz, 12H, H_{cym}), 5.45 (d, 12H, H_{cym}), 5.26 (s, 2H, H^{27}), 5.06 (s, 4H, H^{22}), 4.99 (s, 8H, H^{17}), 4.88 (s, 4H, $H^{17'}$), 3.94 (m, 18H, H^{12} and $H^{12'}$), 2.78 (sept, $^3J_{H-H}=7.0$ Hz, 6H, $CH(CH_3)_2$), 2.57 (m, 2H, H^{31}), 2.01 (s, 18H, CH_3), 1.73 (m, 16H, H^{29}, H^{30}, H^{11} and $H^{11'}$), 1.45 (m, 12H, H^{10} and $H^{10'}$), 1.28 (m, 132H, $H_{aliphatic}$ and $CH(CH_3)_2$), 0.88 ppm (m, 18H, H^1 and $H^{1'}$). $^{13}C\{^1H\}$ NMR (100 MHz, CD_2Cl_2): $\delta=175.6$ (C^{28}), 171.3 (CO), 170.7 (C_{tpt}), 160.1 (C^{24}), 159.6 (C^{13}), 159.4 ($C^{13'}$), 153.5 ($C^{19'}$), 153.2 (C_α), 151.4 (C_{tpt}), 139.3 (C^{18}), 139.2 (C^{26}), 138.0 (CH_{donq}), 133.2 (C^{21}), 130.5 ($C^{15'}$), 130.1 ($C^{16'}$), 129.8 (C^{15}), 129.3 (C^{16}), 124.8 (C_β), 123.1 (CH_{pyr}), 122.6 (CH_{pyr}), 119.9 (CH_{pyr}), 119.7 (C_{pyr}), 119.5 (C_{pyr}), 114.8 (C^{14}), 114.4 ($C^{14'}$), 111.9 (C_{donq}), 108.2 (C^{23}), 108.0 (C^{25}), 107.4 (C^{20}), 104.4 (C_{cym}), 100.5 (C_{cym}), 85.0 (CH_{cym}), 83.2 (CH_{cym}), 75.4 ($C^{17'}$), 71.4 (C^{17}), 68.5 (C^{12}), 68.4 ($C^{12'}$), 32.3 (C^{26}), 31.1 (C^3 and $C^{3'}$), 30.1 ($CH(CH_3)_2$), 30.0 (C_{aliph}), 26.5 (C^{10} and $C^{10'}$), 23.1 (C^2 and $C^{2'}$), 22.4 ($CH(CH_3)_2$), 17.5 (CH_3), 14.3 ppm (C^1 and $C^{1'}$). ESI-MS: m/z 1794.6 $[P_2+\mathbf{1}+(CF_3SO_3)_3]^{3+}$. Elemental analysis calcd (%) for $C_{287}H_{334}F_{18}N_{12}O_{46}Ru_6S_6$: C 59.14, H 5.78, N 2.88; found: C 58.40, H 6.15, N 2.63.

Culture and Inhibition of Cell Growth

Human A2780 and A2780cisR ovarian carcinoma cells were obtained from the European Centre of Cell Cultures (ECACC, Salisbury, UK) and maintained in culture as described by the provider. The cells were routinely grown in RPMI 1640 medium with GlutaMAX™ containing 5% fetal calf serum (FCS) and antibiotics (penicillin and ciproxin) at 37 °C and 5% CO_2. To evaluate the growth inhibition, the cells were seeded in 96-well plates (25×10^3 cells per well) and grown for 24 h in complete medium. Complexes were added to the required concentration and added to the cell culture for 72 h incubation. Solutions of the compounds were applied by diluting a freshly prepared stock solution of the corresponding compound in aqueous RPMI medium with GlutaMAX™ (20 mM). Following drug exposure, 3-(4,5-dimethylthiazol-2-yl)-2,5-diphenyltetrazolium bromide (MTT) was added to the cells at a final concentration of 0.25 mg mL^{-1} and incubated for 2 h, then the culture medium was aspirated and the violet formazan (artificial chromogenic precipitate of the reduction of tetrazolium salts by dehydrogenases and reductases) dissolved in dimethyl sulfoxide (DMSO). The optical density of each well (96-well plates) was quantified three times in triplicates at 540 nm using a multiwell plate reader (iEMS Reader MF, Labsystems, US), and the percentage of surviving cells was calculated from the ratio of absorbance of treated to untreated cells. The IC_{50} values for the inhibition of cell growth were determined by fitting the plot of the logarithmic percentage of surviving cells against the logarithm of the drug concentration using a linear regression function. The median value and the median absolute deviation were obtained from the Microsoft Excel software and those values are reported in Table 2.

Acknowledgements

R.D. thanks the Swiss National Science Foundation (Grant No 200020-129501) for financial support. A generous loan of ruthenium chloride hydrate from the Johnson Matthey Technology Centre is gratefully acknowledged.

[1] a) D. Astruc, E. Boisselier, C. Ornelas, *Chem. Rev.* **2010**, *110*, 1857–1859; b) O. Rolland, C.-O. Turrin, A.-M. Caminade, J.-P. Majoral, *New J. Chem.* **2009**, *33*, 1809–1824; c) S. M. Grayson, J. M. J. Fréchet, *Chem. Rev.* **2001**, *101*, 3819–3868; d) G. R. Newkome, C. Shreiner, *Chem. Rev.* **2010**, *110*, 6338–6442; e) B. M. Rosen, C. J. Wilson, D. A. Wilson, M. Peterca, M. R. Imam, V. Percec, *Chem. Rev.* **2009**, *109*, 6275–6540.

[2] a) A. W. Bosman, H. M. Janssen, E. W. Meijer, *Chem. Rev.* **1999**, *99*, 1665–1688; b) J. W. Goodby, I. M. Saez, S. J. Cowling, V. Görtz, M. Draper, A. W. Hall, S. Sia, G. Cosquer, S.-E. Lee, E. P. Raynes, *Angew. Chem.* **2008**, *120*, 2794–2828; *Angew. Chem. Int. Ed.* **2008**, *47*, 2754–2787; c) T. Kato, N. Mizoshita, K. Kishimoto, *Angew. Chem.* **2006**, *118*, 44–74; *Angew. Chem. Int. Ed.* **2006**, *45*, 38–68.

[3] G. R. Newkome, Z. Yao, G. R. Baker, V. K. Gupta, *J. Org. Chem.* **1985**, *50*, 2003–2004.

[4] a) D. A. Tomalia, H. Baker, J. Dewald, M. Hall, G. Kallos, S. Martin, J. Roeck, J. Ryder, P. Smith, *Polym. J.* **1985**, *17*, 117–132; b) D. A. Tomalia, *Prog. Polym. Sci.* **2005**, *30*, 294–324.

[5] C. J. Hawker, J. M. J. Fréchet, *J. Am. Chem. Soc.* **1990**, *112*, 7638–7647.

[6] M. A. Carnahan, M. W. Grinstaff, *Macromolecules* **2006**, *39*, 609–616.

[7] a) V. Percec, M. Peterca, Y. Tsuda, B. M. Rosen, S. Uchida, M. R. Imam, G. Ungar, P. A. Heiney, *Chem. Eur. J.* **2009**, *15*, 8994–9004; b) B. Donnio, S. Buathong, I. Bury, D. Guillon, *Chem. Soc. Rev.* **2007**, *36*, 1495–2513; c) I. M. Saez, J. W. Goodby, *J. Mater. Chem.* **2005**, *15*, 26–40.

[8] a) G. R. Newkome, E. He, C. N. Moorefield, *Chem. Rev.* **1999**, *99*, 1689–1746; b) D. Astruc, C. Ornelas, J. Ruiz, *Chem. Eur. J.* **2009**, *15*, 8936–8944; c) S. Frein, F. Camerel, R. Ziessel, J. Barberá, R. Deschenaux, *Chem. Mater.* **2009**, *21*, 3950–3959.

[9] a) M. A. Mintzer, M. W. Grinstaff, *Chem. Soc. Rev.* **2011**, *40*, 173–190; b) S. H. Medina, M. E. H. El-Sayed, *Chem. Rev.* **2009**, *109*, 3141–3157.

[10] C. Z. Chen, N. C. Beck-Tan, P. Dhurjati, T. K. van Dyk, R. A. LaRossa, S. L. Cooper, *Biomacromolecules* **2000**, *1*, 473–480.

[11] A. Pérez-Anes, G. Spataro, Y. Coppel, C. Moog, M. Blanzat, C.-O. Turrin, A.-M. Caminade, I. Rico-Lattes, J.-P. Majoral, *Org. Biomol. Chem.* **2009**, *7*, 3491–3498.

[12] R. G. Denkewalter, J. Kolc, W. J. Lukasavage, US Pat. 4289872, **1981**.

[13] E. Buhleier, W. Wehner, F. Vögtle, *Synthesis* **1978**, 155–158.

[14] H. Ihre, A. Hult, E. Söderlind, *J. Am. Chem. Soc.* **1996**, *118*, 6388–6395.

[15] a) M. E. Fox, F. C. Szoka, J. M. J. Fréchet, *Acc. Chem. Res.* **2009**, *42*, 1141–1151; b) M. T. Morgan, Y. Nakanishi, D. J. Kroll, A. P. Griset, M. A. Carnahan, M. Wathier, N. H. Oberlies, G. Manikumar, M. C. Wani, M. W. Grinstaff, *Cancer Res.* **2006**, *66*, 11913–11921; c) M. F. Neerman, H.-T. Chen, A. R. Parrish, E. E. Simanek, *Mol. Pharm.* **2004**, *1*, 390–393; d) A. K. Patri, J. F. Kukowska-Latallo, J. R. Baker, Jr., *Adv. Drug Delivery Rev.* **2005**, *57*, 2203–2214.

[16] a) B. A. J. Jansen, J. van der Zwan, J. Reedijk, H. den Dulk, J. Brouwer, *Eur. J. Inorg. Chem.* **1999**, 1429–1433; b) T. Kapp, A. Dullin, R. Gust, *J. Med. Chem.* **2006**, *49*, 1182–1190; c) W. H. Ang, E. Daldini, L. Juillerat-Jeanneret, P. J. Dyson, *Inorg. Chem.* **2007**, *46*, 9048–9050; d) P. Govender, N. C. Antonels, J. Mattsson, A. K. Renfrew, P. J. Dyson, J. R. Moss, B. Therrien, G. S. Smith, *J. Organomet. Chem.* **2009**, *694*, 3470–3476; A. Ruggi, C. Beekman, D. Wasserberg, V. Subramaniam, D. N. Reinhoudt, F. W. B. van Leeuwen, A. H. Velders, *Chem. Eur. J.* **2011**, *17*, 464–467.

[17] a) V. S. K. Balagurusamy, G. Ungar, V. Percec, G. Johansson, *J. Am. Chem. Soc.* **1997**, *119*, 1539–1555; b) V. Percec, W.-D. Cho, G. Ungar, D. J. P. Yeardley, *J. Am. Chem. Soc.* **2001**, *123*, 1302–1315.

[18] a) V. Percec, G. Johansson, J. Heck, G. Ungar, S. V. Batty, *J. Chem. Soc. Perkin Trans. 1* **1993**, 1411–1420; b) G. Johansson, V. Percec, G. Ungar, D. Abramic, *J. Chem. Soc. Perkin Trans. 1* **1994**, 447–459.

[19] a) N. P. E. Barry, B. Therrien, *Eur. J. Inorg. Chem.* **2009**, 4695–4700; b) J. Freudenreich, N. P. E. Barry, G. Süss-Fink, B. Therrien, *Eur. J. Inorg. Chem.* **2010**, 2400–2405.

[20] a) B. Therrien, G. Süss-Fink, P. Govindaswamy, A. K. Renfrew, P. J. Dyson, *Angew. Chem.* **2008**, *120*, 3833–3836; *Angew. Chem. Int. Ed.* **2008**, *47*, 3773–3776; b) J. Mattsson, P. Govindaswamy, J. Furrer, Y. Sei, K. Yamaguchi, G. Süss-Fink, B. Therrien, *Organometallics* **2008**, *27*, 4346–4356; c) J. Mattsson, O. Zava, A. K. Renfrew, Y. Sei, K. Yamaguchi, P. J. Dyson, B. Therrien, *Dalton Trans.* **2010**, *39*, 8248–8255.

[21] A. Pitto-Barry, N. P. E. Barry, O. Zava, R. Deschenaux, P. J. Dyson, B. Therrien, *Chem. Eur. J.* **2011**, *17*, 1966–1971.

[22] a) O. Zava, J. Mattsson, B. Therrien, P. J. Dyson, *Chem. Eur. J.* **2010**, *16*, 1428–1431; b) P. Govindaswamy, D. Linder, J. Lacour, G. Süss-Fink, B. Therrien, *Chem. Commun.* **2006**, 4691–4693.

[23] a) K. S. Singh, V. Svitlyk, Y. Mozharivskyj, *Dalton Trans.* **2011**, *40*, 1020–1023; b) H. Yan, G. Süss-Fink, A. Neels, H. Stoeckli-Evans, *J. Chem. Soc. Dalton Trans.* **1997**, 4345–4350.

[24] D. Schweinfurth, H. Sankar Das, F. Weisser, D. Bubrin, B. Sarkar, *Inorg. Chem.* **2011**, *50*, 1150–1159.

[25] *HyperChem*. Computational Chemistry Software Package Version 7.5, Hypercube Inc., Gainesville, Florida, **2003**.

[26] a) Y. Kikuchi, Y. Kato, Y. Tanaka, H. Toi, Y. Aoyama, *J. Am. Chem. Soc.* **1991**, *113*, 1349–1354; b) L. Fielding, *Tetrahedron* **2000**, *56*, 6151–6170.

[27] M. J. Hynes, *J. Chem. Soc. Dalton Trans.* **1993**, 311–312.

[28] K. A. Connors in *Binding Constants*, Wiley, New York, **1987**, pp. 141.

[29] H. Tsukube, H. Furuta, A. Odani, Y. Takeda, Y. Kudo, Y. Inoue, Y. Liu, H. Sakamoto, K. Kimura, in *Comprehensive Supramolecular Chemistry, Vol. 8* (Eds.: J. L. Atwood, J. E. D. Davies, D. D. MacNi-

col, F. Vögtle, J.-M. Lehn, J. A. Ripmeester), Pergamon Press, Oxford, **1996**, pp. 425.

[30] a) E. Wong, C. M. Giandomenico, *Chem. Rev.* **1999**, *99*, 2451–2466; b) N. J. Wheate, S. Walker, G. E. Craig, R. Oun, *Dalton Trans.* **2010**, *39*, 8113–8127.

[31] a) C. G. Hartinger, S. Zorbas-Seifried, M. A. Jakupec, B. Kynast, H. Zorbas, B. K. Keppler, *J. Inorg. Biochem.* **2006**, *100*, 891–904; b) C. G. Hartinger, M. A. Jakupec, S. Zorbas-Seifried, M. Groessl, A. Egger, W. Berger, H. Zorbas, P. J. Dyson, B. K. Keppler, *Chem. Biodiversity* **2008**, *5*, 2140–2155; c) S. Pacor, S. Zorzet, M. Cocchietto, M. Bacac, M. Vadori, C. Turrin, B. Gava, A. Castellarin, G. Sava, *J. Pharmacol. Exp. Ther.* **2004**, *310*, 737–744; d) G. Sava, S. Zorzet, C. Turrin, F. Vita, M. Soranzo, G. Zabucchi, M. Cocchietto, A. Bergamo, S. DiGiovine, G. Pezzoni, L. Sartor, S. Garbisa, *Clin. Cancer Res.* **2003**, *9*, 1898–1905.

[32] a) W. H. Ang, P. J. Dyson, *Eur. J. Inorg. Chem.* **2006**, 4003–4018; b) P. J. Dyson, *Chimia* **2007**, *61*, 698–703; c) G. Süss-Fink, *Dalton Trans.* **2010**, *39*, 1673–1688.

[33] a) D. F. Baban, L. W. Seymour, *Adv. Drug Delivery Rev.* **1998**, *34*, 109–119; b) S. Modi, J. P. Jain, A. J. Domb, N. Kumar, *Curr. Pharm. Des.* **2006**, *12*, 4785–4796.

[34] a) P. Govender, A. K. Renfrew, C. M. Clavel, P. J. Dyson, B. Therrien, G. S. Smith, *Dalton Trans.* **2011**, *40*, 1158–1167; b) A. L. Hurley, D. L. Mohler, *Org. Lett.* **2000**, *2*, 2745–2748; c) X. Zhao, S. C. J. Loo, P. P.-F. Lee, T. T. Y. Tan, C. K. Chu, *J. Inorg. Biochem.* **2010**, *104*, 105–110; d) N. Malik, E. G. Evagorou, R. Duncan, *Anti-Cancer Drugs* **1999**, *10*, 767–776.

[35] Y. Niu, R. M. Crooks in *Dendrimers and Nanoscience*, *Vol. 6* (Ed.: D. Astruc), Compte-Rendus Chimie, Elsevier, Paris, **2003**, pp. 989.

[36] H.-B. Yang, N. Das, F. Huang, A. M. Hawkridge, D. C. Muddiman, P. J. Stang, *J. Am. Chem. Soc.* **2006**, *128*, 10014–10015.

[37] W. H. Ang, A. Casini, G. Sava, P. J. Dyson, *J. Organomet. Chem.* **2011**, *696*, 989–998.

[38] a) S. C. Srivastava, P. Richards, G. E. Meinken, S. M. Larson, Z. Grunbaum, in *Radiopharmaceuticals—Structures—Activity relationships* (Ed.: R. P. Spencer) Grune&Stratton Inc., New York, **1981**, pp. 207; b) C. Scolaro, A. Bergamo, L. Brescacin, R. Delfino, M. Cocchietto, G. Laurenczy, T. J. Geldbach, G. Sava, P. J. Dyson, *J. Med. Chem.* **2005**, *48*, 4161–4171.

[39] H. L. Anderson, S. Anderson, J. K. M. Sanders, *J. Chem. Soc. Perkin Trans. 1* **1995**, 2231–2245.

[40] J. S. Moore, S. I. Stupp, *Macromolecules* **1990**, *23*, 65–70.

[41] G. M. Sheldrick, *Acta Crystallogr. Sect. A* **2008**, *64*, 112–122.

[42] L. J. Farrugia, *J. Appl. Crystallogr.* **1997**, *30*, 565.